Saturation of the All-Optical Kerr Effect

Carsten Brée,[1,2] Ayhan Demircan,[1] and Günter Steinmeyer[2,3]

[1]*Weierstraß-Institut für Angewandte Analysis und Stochastik, 10117 Berlin, Germany*
[2]*Max-Born-Institut für Nichtlineare Optik und Kurzzeitspektroskopie, 12489 Berlin, Germany*
[3]*Optoelectronics Research Centre, Tampere University of Technology, 33101 Tampere, Finland*

(Received 24 September 2010; published 3 May 2011)

Saturation of the intensity dependence of the refractive index is directly computed from ionization rates via a Kramers-Kronig transform. The linear intensity dependence and its dispersion are found to be in excellent agreement with complete quantum mechanical orbital computations. Higher-order terms concur with solutions of the time-dependent Schrödinger equation. Expanding the formalism to all orders up to the ionization potential of the atom, we derive a model for saturation of the Kerr effect. This model widely confirms recently published and controversially discussed experimental data and corroborates the importance of higher-order Kerr terms for filamentation.

DOI: 10.1103/PhysRevLett.106.183902 PACS numbers: 42.65.Tg, 42.68.Ay, 52.38.Hb

Most nonlinear optical effects can be understood in the perturbative limit with two or three interacting optical waves, giving rise to contributions $\chi^{(2)}_{ij}E_iE_j$ or $\chi^{(3)}_{ijk}E_iE_jE_k$ to the polarization P, respectively. Higher-order $\chi^{(n)}$ ($n \geq 4$) terms can be formally considered. Yet, a perturbative description of higher-order effects is rarely useful as often enough a large number of waves interact simultaneously as, for example, in high-harmonic generation [1]. The role of $\chi^{(5)}$ effects for arresting catastrophic optical self-focusing has been discussed already more than 20 years ago [2–4]. $\chi^{(3)}$ effects, namely, the all-optical Kerr effect, give rise to an increase of the refractive index with intensity $n = n_0 + n_2 I$ and a resulting focusing nonlinear lens. A $\chi^{(5)}$ dependence with negative sign and defocusing nonlinear lensing would explain the phenomenon of filamentation, i.e., the formation of long self-guided light strings with nearly constant diameter. Early experimental results indicated that filamentation cannot only be explained by plasma formation [5], which gives rise to a negative index contribution suitably described by Drude theory. Nevertheless, refined theoretical models succeeded in explaining even complex experimental results without the need for including a saturation of the Kerr effect [6,7]. Recently, this accepted picture was challenged by measurements [8,9] that indicate yet again a strong influence of higher-order nonlinearities to the extent that filament formation is explained in the complete absence of plasma formation. These results have been controversially discussed [10,11]. In the following, we provide an independent and previously unreported approach towards computing Kerr saturation. Our approach is based on a Kramers-Kronig (KK) transform [12] of optical absorption derived from Keldysh theory [13]. This analysis supports the experimental results in Ref. [8], indicating that we may have in fact a paradigm shift in explaining femtosecond filamentation [10].

Our model is based on a recent modification [13] of Perelomov-Popov-Terent'ev (PPT) theory [14], the former providing cross sections for multiphoton ionization (MPI) according to

$$\sigma_K(\omega) = \frac{2\sqrt{2}C^2}{\pi}(2e)^{2n^*}\left(\frac{e}{2}\right)^{2K}\omega_p^{-3K+1}\left(\frac{q_e^2}{\hbar m_e \epsilon_0 c}\right)^K \times \left(\frac{\omega_p}{\omega}\right)^{2n^*+2K-(3/2)}\exp\left(-\frac{\omega_p}{\omega}\right)w_0\left[\sqrt{2K-2\frac{\omega_p}{\omega}}\right], \quad (1)$$

for $\omega \geq \omega_p/K$. Here ω is the optical frequency, q_e and m_e denote electron charge and mass, respectively, ϵ_0 is the vacuum dielectric constant, and c denotes vacuum light speed. $\hbar\omega_p$ is the ionization potential of the gas species under consideration. The constant $K = \langle \omega_p/\omega + 1 \rangle$ counts the number of photons required for ionization, where $\langle x \rangle$ denotes the integer part of x. The effective principal quantum number of the bound state is given by $n^* = Z\sqrt{\omega_H/\omega_p}$, where $\hbar\omega_H = 13.6$ eV is the Rydberg energy and Z is the charge number of the ionic residuum. The constant $C = 2^{n^*-1}/\Gamma(n^* + 1)$ is related to the asymptotic expansion of the ground-state electronic wave function, and $w_0[x]$ denotes Dawson's function [15]. From the cross sections σ_K, the K-photon absorption coefficients $\Delta\alpha_K$ may then be calculated according to $\Delta\alpha_K(\omega) = K\hbar\omega\rho_{\mathrm{nt}}\sigma_K I^{K-1}$, with a particle density $\rho_{\mathrm{nt}} = 2.7 \times 10^{19}\ \mathrm{cm}^{-3}$ corresponding to standard conditions. For atomic argon, this perturbative approximation is expected to hold for intensities up to 50 TW/cm^2. This intensity corresponds to a Keldysh parameter of $\gamma = 1.62$, where MPI is the dominant ionization channel [16].

Kramers-Kronig theory has been successfully applied to nonlinear refraction in solids [12,17]. Here we combine this method with Keldysh theory to compute nonlinear refraction in inert gases. In principle, as pointed out in

[12], the use of the KK relation requires knowledge of nondegenerate multiphoton absorption coefficients $\Delta\alpha_K^N(\omega_1, \ldots, \omega_K)$. These coefficients cannot easily be provided by PPT theory. Instead, we use

$$\Delta\alpha_K^N(\omega_1, \ldots, \omega_K) = \Delta\alpha_K\left(\frac{\omega_1 + \ldots + \omega_K}{K}\right) \quad (2)$$

as an estimate, generalizing the model successfully used to compute n_2 in solids [17].

Using this proven simplification, we find that the nonlinear refraction coefficients n_{2k} are related to $(k+1)$-photon absorption coefficients σ_{k+1} via the KK relation according to

$$n_{2k}(\omega) = \frac{\hbar c \rho_{\mathrm{nt}}}{\pi} \fint_0^\infty (\Omega + k\omega) \frac{\sigma_{k+1}(\frac{\Omega+k\omega}{k+1})}{\Omega^2 - \omega^2} d\Omega, \quad (3)$$

where $\fint$ denotes Cauchy's principal value integral. It has been shown in Ref. [17] that Eq. (2) is a reasonable approximation when ac Stark terms are neglected in the model. As a benchmark for our model, we calculate the leading term $n_2(\omega)$ of nonlinear refraction for helium [Fig. 1], setting $k = 1$.

Among the inert gases, helium is the least complex atom and the only one for which detailed computations of n_2 from atomic wave functions exist. For large wavelengths, our analysis indicates a value $n_2 = 4.8 \times 10^{-9}$ cm^2/TW, which deviates by only 26% from the value 3.8×10^{-9} cm^2/TW that was derived in [18] using explicitly electron-correlated wave functions. Keeping in mind that the absorption spectra σ_K have been derived from strong field ionization rates for which often an order of magnitude agreement with experimental data is considered reasonable, our KK approach provides an excellent prediction of n_2. Our model also correctly reproduces the dispersive behavior of n_2 predicted in Ref. [18] and reasonably agrees with experimental data at 1.06 μm wavelength [19]. Even better agreement is obtained for argon [Fig. 2]. Going beyond the tabulated values of [18] for helium, our computations predict that n_2 reaches a maximum value $n_2 \approx 4 \times 10^{-8}$ cm^2/TW at about 100 nm wavelength, which corresponds to half the ionization energy. Going to even smaller wavelengths, n_2 crosses zero at 85 nm and stays negative up to the ionization energy equivalent of 50.4 nm wavelength. This prototypical behavior with a sign change at approximately 60% of the ionization threshold is seen for all inert gases and duplicates the dispersion characteristics of n_2 in solids [17]. Compared to our previous work [20], the possibility to extend n_2 computation beyond half the ionization energy into the negative region and the correct prediction of its dispersion in the positive region both arise from usage of the improved ionization cross sections provided in Ref. [13].

Similarly good agreement of Eq. (3) with independent experimental and theoretical data is obtained for neon, krypton, and xenon, for which our approach reproduces experimental and theoretical data [21,22] within 15% precision.

Figure 2 shows an n_2 computation for argon showing similar features as the helium example. Given that the ionization energy of argon is only 15.76 eV and that a smaller number of photons is required to reach the continuum, n_2 of argon is about a factor of 20 larger in the infrared, with a value of $\approx 10^{-7}$ cm^2/TW. This value agrees favorably with commonly used reference data [19] and was also reproduced by Loriot *et al.* in their measurements. Compared to helium, the zero crossing of n_2 is now shifted to a wavelength of 140 nm.

Nonlinear refraction, in principle, holds two potential mechanisms for saturation. First, the generation of free electrons will replace a number of neutral atoms by ions. In the case of Ar^+, this raises the ionization threshold to 27.63 eV, which, in turn, has to reduce the resulting n_2 values as illustrated by the transition from argon to helium. A computation of the resulting values for Ar^+ is shown as the dashed line in Fig. 2(b), which confirms a reduction of n_2 by a factor of ≈ 2. Table I lists computed values of n_2 of all noble gases and their first ionic species ($Z = 1, 2$) for 800 nm wavelength.

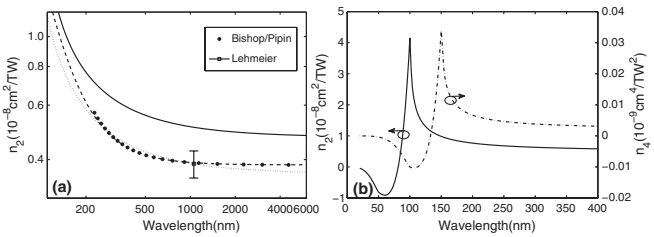

FIG. 1. (a) Nonlinear refractive index n_2 of He below the two-photon absorption (TPA) resonance at $\lambda = 85$ nm. Solid lines: n_2 dispersion as extracted from Eq. (3). Dashed line: fit of theoretical data to scaling law (dots) from [21]. (b) Same in the vicinity of the resonance (solid line), dash-dotted line showing $n_4(\omega)$.

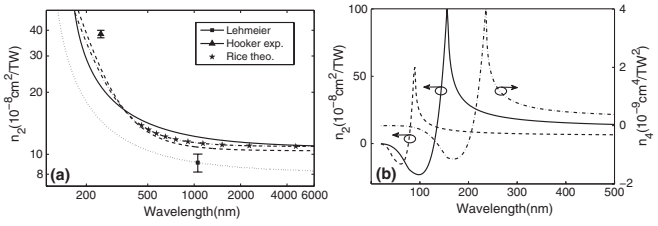

FIG. 2. (a) Nonlinear refractive index n_2 of Ar below the TPA resonance. Solid line: KK approach, Eq. (3). Dash-dotted line: power series in ω^2 [21,22] fitted to theoretical data [22] (stars). Dashed line: experimental n_2 data [21]. Dotted line: Lehmeier data extrapolated with scaling law given in [19]. (b) n_2 of neutral argon in the vicinity of the TPA resonance at $\lambda = 85$ nm [solid line, Eq. (3)]. Dashed line: n_2 of singly ionized Ar^+. Dash-dotted line: $n_4(\omega)$ for Ar.

TABLE I. Nonlinear refractive index n_2 for neutral noble gases in the static limit $n_2(\omega \to 0)$ and at 800 nm ($Z = 1$) as well as for simply ionized atoms ($Z = 2$). Experimental data (rightmost column) as compiled from [18,21] and corrected for the dispersion of the DFWM process with Eq. (13) in [20].

	n_2 (10^{-8} cm^2/TW)			
Element	$Z = 1$	$Z = 2$	$n_2(\omega \to 0)$	Refs. [18,21]
He	0.52	0.03	0.48	0.38
Ne	1.31	0.27	1.18	0.96
Ar	12.68	6.14	10.84	10.40
Kr	30.69	17.28	25.63	23.17
Xe	91.58	55.17	73.87	61.39

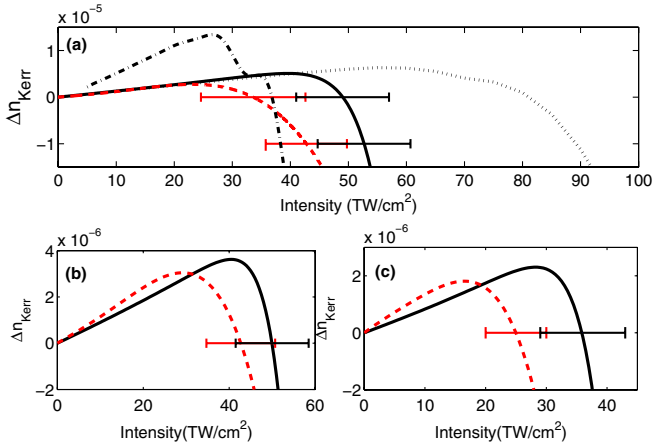

FIG. 3 (color online). Kerr saturation in (a) argon, (b) nitrogen, and (c) oxygen at 800 nm due to higher-order Kerr terms [Eq. (3), solid lines], classical filamentation model due to plasma clamping (dotted line), and experimental results [8] (dashed lines). Dash-dotted line in (a) depicts TDSE results for argon found in [26].

While this first mechanism suggests a depletion of the neutral atoms as the cause for saturation, the same effect may also occur due to higher-order Kerr terms n_{2k} with $k \geq 2$. These terms can also be computed using our theoretical approach. As an example, we have plotted $n_4(\omega)$ of helium and argon as dash-dotted lines in Figs. 1(b) and 2(b), respectively. According to our model, argon displays an infrared limit $n_4(\omega \to 0) = 2 \times 10^{-12}$ cm^4/TW^2, reaches a 12 times higher maximum value at 240 nm, and is negative below 210 nm. This behavior is again in agreement with the prototypical dispersion of the Kerr coefficients, yet caused by three-photon rather than two-photon absorption.

There is an apparent contradiction to the negative value $n_4 = -0.36 \pm 1.03 \times 10^{-9}$ cm^4/TW^2 reported in Ref. [8]. In principle, a negative n_4 value at 800 nm appears to be incompatible with the dispersion of the Kerr terms predicted by our model.

The analysis of higher-order Kerr terms can easily be continued to arbitrary order k in our model, even beyond the highest-order experimental n_{10} term in Ref. [8]. Again, helium provides a benchmark for this extension. Using the theoretical susceptibility data published in Ref. [23], we find excellent (within 10%) agreement with n_4 and n_6 values derived from KK theory. The agreement only breaks down in the highest-order coefficient n_{10} extracted from the series expansion used in Ref. [23].

For argon at a wavelength of 800 nm, we compute positive coefficients up to n_{18}. Higher-order coefficients are negative and merge into a series with constant ratio between successive coefficients [24]. This geometric series ensures convergence up to 70 TW/cm^2. Despite the nonalternating structure of our sequence of Kerr coefficients, we find a good agreement between the computed nonlinearly induced index change $\Delta n_{\mathrm{Kerr}} = n_2 I + n_4 I^2 + n_6 I^3 + \ldots$ and the experimental values for argon in [8], see Fig. 3(a). Our model predicts an increase of Δn_{Kerr} up to about 42 TW/cm^2 and inversion of the index change at 49 TW/cm^2. This is contrasted by experimental values of 30 and 34 TW/cm^2, respectively. Apart from this apparent scaling issue, both curves agree remarkably well within the error bounds. These bounds have been extracted from the uncertainty of the experimental Kerr coefficients given in Ref. [8]. In contrast, the error of our theoretical values has been estimated from the comparison of our benchmark n_2 values with independent values in the literature.

From the coefficients for He, Ne, Kr, and Xe shown in [24], we deduce inversion intensities of 112, 89, 40, and 30 TW/cm^2, respectively. Our analysis also qualitatively agrees with solutions of the time-dependent Schrödinger equation (TDSE) for atomic hydrogen [25]. Agreement with corresponding calculations for argon performed in Ref. [26] is shown by the dash-dotted curve in Fig. (3), indicating a favorable agreement of the inversion intensity within reasonable error margins. For the air constituents O_2 and N_2, Figs. 3(b) and 3(c) show the experimentally measured $\Delta n_{\mathrm{Kerr}}(I)$ in comparison to our theoretical derivations. In order to apply the PPT model to molecular gases, we employ the semiempirical model of Ref. [27] with $Z_{\mathrm{eff}} = 0.53$ and 0.9 for O_2 and N_2, respectively. For oxygen, our theory yields a long-wavelength limit $n_2(\omega \to 0) = 0.7 \times 10^{-7}$ cm^2/TW, which agrees excellently with the electronic contribution of $n_2 = 0.746 \times 10^{-7}$ cm^2/TW computed in [28].

Despite delivering a higher inversion intensity than reported in [8], our model nevertheless confirms plasma clamping to occur at significantly higher intensities than Kerr saturation. Figure 3(a) shows the refractive index change $\Delta n(I) = n_2 I - \rho/2\rho_c$ induced by second-order nonlinear refraction and the generation of free electrons with density ρ under experimental conditions of [8]. $\rho_c = m_e \epsilon_0 \omega^2 / q_e^2$ is the critical plasma density. Clearly, plasma clamping is expected at intensities beyond ≈ 80 TW/cm^2, i.e., well above Kerr saturation.

In a second simulation, we model the potential effect of depletion of neutral atoms on the index change.

Given a fraction p of ionized atoms, we compute $n_2(I) = pn_{2,\mathrm{Ar}^+} + (1-p)n_{2,\mathrm{Ar}}$ where p is computed under the assumption of 90 fs Gaussian pulses with peak intensity I using the ionization model of [13], duplicating experimental conditions of Ref. [8]. In this case we yield a classical saturation behavior (not shown), yet at much higher intensities $I > 250$ TW/cm^2 and without any index inversion. Complete ionization of argon requires intensities of $\sim$300 TW/cm^2, and even then only a 50% index change from $n_2 = 1.3 \times 10^{-7}$ cm^2/W at $p = 0$ to $n_2 = 0.6 \times 10^{-7}$ cm^2 at $p = 1$ results. As this happens nearly an order of magnitude beyond the inversion intensities discussed previously, depletion effects can be clearly ruled out.

These results shed new light on the long-disputed mechanism behind filament formation. First and foremost, saturation of the Kerr effect cannot be explained by inclusion of the next higher-order coefficient n_4 alone. Instead, similar as in the transition from third-harmonic generation to high-harmonic generation, many coefficients start to act simultaneously. Nevertheless, the assumptions of perturbative nonlinear optics are expected to hold as long as the intensity does not exceed the validity of the MPI regime. Beyond that regime, a perturbative expansion of the ionization rate provided by PPT ceases to exist.

While a true depletion-caused saturation $n_2(I) = n_2(0)/(1 + I/I_{\mathrm{sat}})$ can be developed into a Taylor series in I resulting in a sequence of n_{2k} with alternating signs, our model predicts that all n_{2k} are positive until the driving $(k+1)$-photon process reaches about 75% of the ionization energy. This causes a nearly unperturbed linear increase of the index change Δn_{Kerr} up to a certain threshold. Above this threshold, Δn_{Kerr} will rapidly decrease and reach strong negative values. Comparing the absolute values of n_4 from our model with Ref. [8], we generally compute smaller values than found in Taylor series analysis of experimental data. This finding corroborates that saturation of the Kerr effect may be perfectly compatible with experimentally observed efficiencies of fifth-order harmonic generation processes [10].

Despite its slightly different functional shape, our results qualitatively confirm the saturation behavior suggested by Loriot *et al.* This agreement strongly suggests to include a saturation mechanism into future models of filament formation. Modeling of white-light propagation, however, may turn out to be difficult because of the strong dispersion of the higher-order coefficients, and methods for efficient modeling of dispersive nonlinearities may have to be found. We believe that this work has important consequences for nonlinear optics in a large class of materials, including gases, solids, and metamaterials. In fact, this may truly induce a paradigm shift in the understanding of filamentation.

Financial support by the Deutsche Forschungsgemeinschaft, Grants No. DE 1209/1-2 and No. STE 762/7-2, is gratefully acknowledged. G. S. gratefully acknowledges support by the Academy of Finland (Project Grant No. 128844).

[1] A. McPherson *et al.*, J. Opt. Soc. Am. B **4**, 595 (1987); X. F. Li, A. L'Huillier, M. Ferray, L. A. Lompré, and G. Mainfray, Phys. Rev. A **39**, 5751 (1989).
[2] J. T. Manassah and M. A. Mustafa, Opt. Lett. **13**, 862 (1988).
[3] A. Vinçotte and L. Bergé, Phys. Rev. A **70**, 061802 (2004).
[4] S. Champeaux, L. Bergé, D. Gordon, A. Ting, J. Peñano, and P. Sprangle, Phys. Rev. E **77**, 036406 (2008).
[5] P. B. Corkum, C. Rolland, and T. Srinivasan-Rao, Phys. Rev. Lett. **57**, 2268 (1986).
[6] S. Skupin *et al.*, Phys. Rev. E **74**, 056604 (2006).
[7] A. L. Gaeta, Phys. Rev. Lett. **84**, 3582 (2000).
[8] V. Loriot *et al.*, Opt. Express **17**, 13 429 (2009); **18**, 3011 (E) (2010).
[9] P. Béjot *et al.*, Phys. Rev. Lett. **104**, 103903 (2010).
[10] M. Kolesik, E. M. Wright, and J. V. Moloney, Opt. Lett. **35**, 2550 (2010).
[11] A. Teleki, E. M. Wright, and M. Kolesik, Phys. Rev. A **82**, 065801 (2010).
[12] D. C. Hutchings *et al.*, Opt. Quantum Electron. **24**, 1 (1992).
[13] S. V. Popruzhenko *et al.*, Phys. Rev. Lett. **101**, 193003 (2008).
[14] A. M. Perelomov, V. S. Popov, and M. V. Terent'ev, Sov. Phys. JETP **23**, 924 (1966).
[15] *Handbook of Mathematical Functions*, edited by M. Abramowitz and I. A. Stegun (Dover, New York, 1972), 9th printing, pp. 295, 319.
[16] M. Abu-samha and L. B. Madsen, J. Phys. B **41**, 151001 (2008); M. Wickenhauser *et al.*, Phys. Rev. A **74**, 041402 (R) (2006).
[17] M. Sheik-Bahae, D. J. Hagan, and E. W. Van Stryland, Phys. Rev. Lett. **65**, 96 (1990); M. Sheik-Bahae, D. C. Hutchings, D. J. Hagan, and E. W. Van Stryland, IEEE J. Quantum Electron. **27**, 1296 (1991).
[18] D. M. Bishop and J. Pipin, J. Chem. Phys. **91**, 3549 (1989).
[19] H. J. Lehmeier, W. Leupacher, and A. Penzkofer, Opt. Commun. **56**, 67 (1985).
[20] C. Brée, A. Demican, and G. Steinmeyer, IEEE J. Quantum Electron. **46**, 433 (2010).
[21] D. P. Shelton and J. E. Rice, Chem. Rev. **94**, 3 (1994).
[22] J. E. Rice, J. Chem. Phys. **96**, 7580 (1992).
[23] W. -C. Liu, Phys. Rev. A **56**, 4938 (1997).
[24] See supplemental material at http://link.aps.org/supplemental/10.1103/PhysRevLett.106.183902 for a compilation of the nonlinear coefficients n_2 to n_{32} of He, Ne, Ar, Kr, and Xe.
[25] M. Nurhuda, A. Suda, and K. Midorikawa, New J. Phys. **10**, 053006 (2008).
[26] M. Nurhuda, A. Suda, K. Midorikawa, RIKEN Rev. **48**, 40 (2002).
[27] A. Talebpour, J. Yang, S. L. Chin, Opt. Commun. **163**, 29 (1999).
[28] R. W. Hellwarth, D. M. Pennington, and M. A. Henesian, Phys. Rev. A **41**, 2766 (1990).